A Heats of formation

compound	ΔH_f^0 / kJmol^{-1} [72]
$C_5H_{10}O_5$ (D-ribose, solid)	-1050
$C_6H_{12}O_6$ (D-fructose, solid)	-1266
H_2O (gas)	-242
CO_2	-394
CH_2O (gas)	-116
H	218
CH_3OH (gas)	-201

Table A.1: Heats of formation of compounds relevant in DEA to sugars.

B Structures of 72 and 101 amu anions

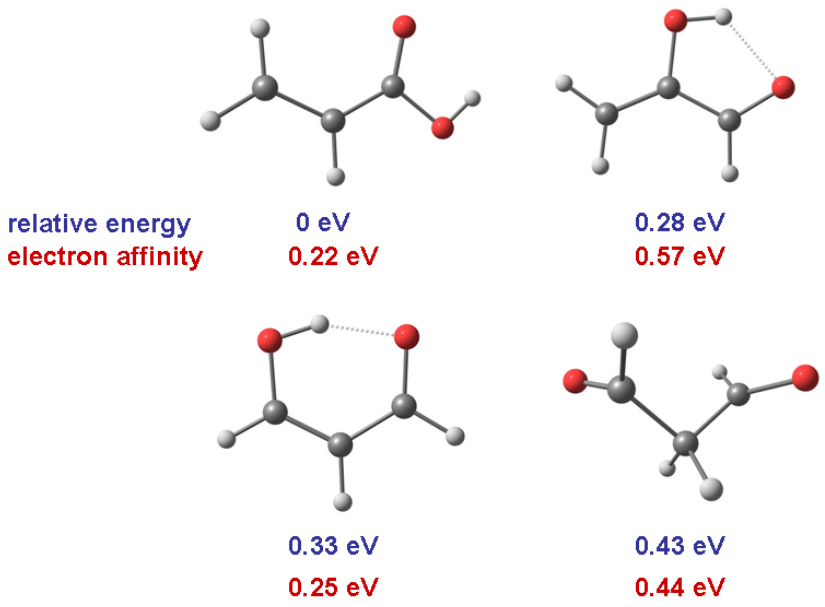

Figure B.1: Four stable anions for the sum formula $C_3H_4O_2^-$ that have been found using DFT calculations at the B3LYP/6-31++G** level. The relative energy of each isomer/conformer is given in blue, the electron affinity (calculated as the difference of relaxed neutral and relaxed anionic electronic energy including ZPE) is given in red. All anionic structures are close in energy and possess comparatively low electron affinities.

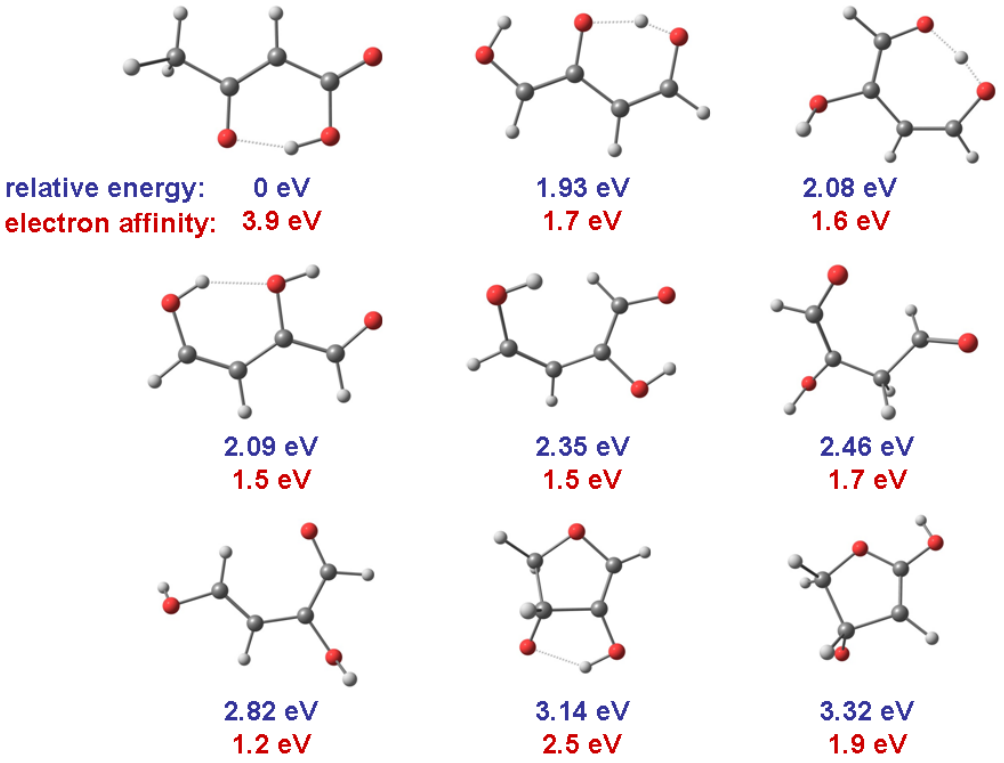

Figure B.2: Stable anionic structures for the sum formula $C_4H_5O_3^-$ according to DFT calculations at the B3LYP/6-31++G** level. The relative energy of each isomer/conformer is given in blue, the electron affinity (calculated as the difference of relaxed neutral and relaxed anionic electronic energy including ZPE) is given in red. It appears that the first structure is the energetically lowest one with an appreciable electron affinity of 3.9 eV. All other anions are higher in energy by at least 1.93 eV.

C Electronic and vibrational excitation of furan by low energy electrons

Monoenergetic electrons can serve as analytical tool to probe vibrational and electronic excitation of molecules by means of electron energy loss spectroscopy (EELS). In the present work the heterocyclic aromatic molecule furan was investigated. Dissociative electron attachment of furan was already investigated in the author's diploma thesis [92, 91] in a comparative study along with the nonaromatic tetrahydrofuran, which is frequently used as a surrogate for a sugar ring.

Furan (C_4H_4O) possesses 21 normal modes, and the point group is C_{2v} due to the planar aromatic ring.

Experiment The experiments have been carried out in the group of Robert Abouaf at LCAM (Laboratoire des collisions atomique et moléculaire), CNRS - Université Paris Sud. A monochromatic electron beam is generated by a double hemispherical electrostatic analyser and crosses an effusive beam of furan molecules. The scattered electrons are energy analysed by a similar double hemispherical analyser and collected by a channeltron. To analyse the angular distribution of scattered electrons the electron energy analyser can be rotated in the range 3° - 90° with respect to the incident electron beam. An energy resolution of 22 -

35 meV was achieved in the electron energy loss mode. Furan is a liquid with sufficient vapour pressure to introduce it at room temperature into the chamber through a needle. The temperature inside the chamber was increased to 130 °C to prevent condensation of furan molecules on the lenses of the analysers.

Electronic excitation The electronic ground state configuration of the valence orbitals of furan is $(9a_1)^2(2b_1)^2(1a_2)^2(3b_1)^0(2a_2)^0$, the latter two orbitals representing the π^* orbitals.

Electronic excitation by electron impact allows a distinction between dipole allowed transitions (for instance singlet-singlet) and singlet-triplet transitions, which are optically forbidden. If the energy of the incident electron is noticeably larger than the excitation energy, the momentum transfer is close to zero and the deviation of the electrons is small. In this case dipole allowed transitions are favoured, that can mainly be observed at small scattering angles.

At lower incident energies the electron penetrates the electron cloud of the molecule and electron interaction takes place leading to a larger deviation of the electrons [119]. Due to the more general electron interaction potential instead of the electric dipole interaction, the optical selection rules are no more valid. By choosing large angles and very low residual energies E_r the singlet states may be suppressed and triplet states can be observed.

The spectra reported here are recorded in the constant residual energy mode, i.e., the residual energy E_r is fixed and the incident energy is varied. Electronic excitation by electron impact has been reported in [120, 121].

The spectrum in figure C.1 is recorded at $E_r = 93\,\text{eV}$ and a scattering angle $\theta = 3.5°$, i.e. primarily singlet excited states are observed and the spectrum is similar to the UV spectrum. The first broad band is assigned to a valence excited state of symmetry $^1B_2$ ($\pi\pi^*$ transition; $a_2b_1^*$). The maximum is at 6.04 eV in agreement with UV-spectra [120] and exhibits a vibrational structure with energy spacings of 110 - 140 meV. The second broad peak is due to a $\pi\pi^*$ transition of symmetry

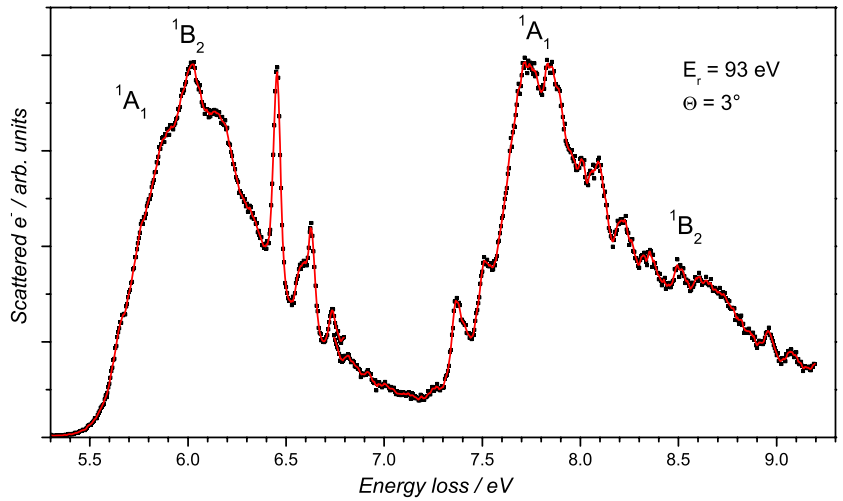

Figure C.1: Electronic excitation of furan, singlet excited states

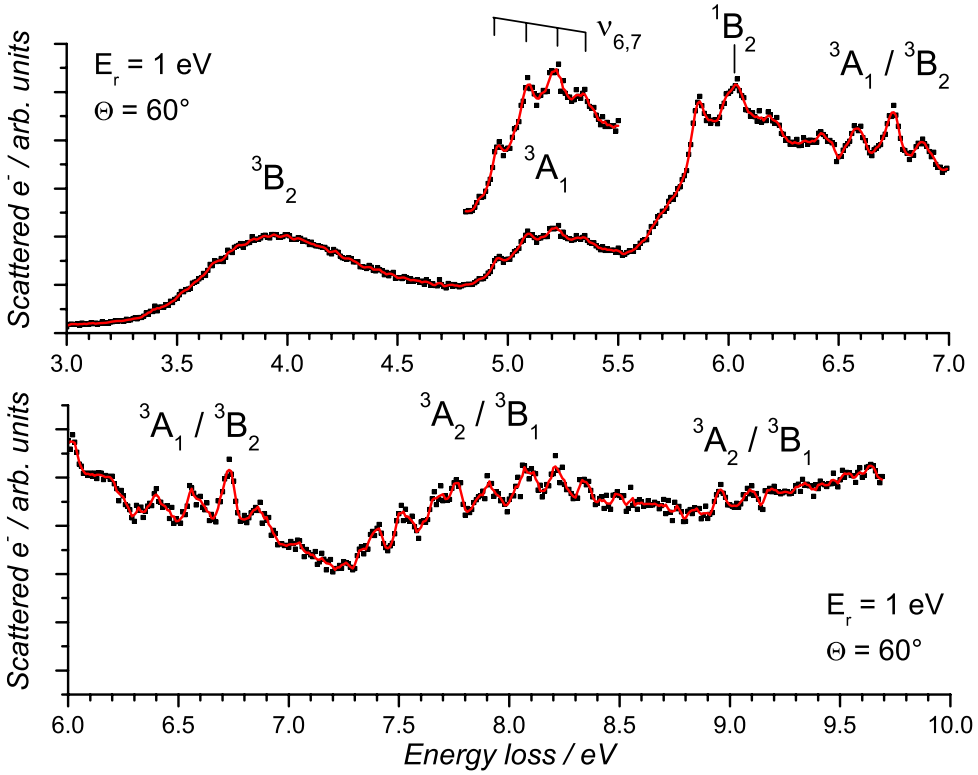

Figure C.2: Electronic excitation of furan at larger angles and small E_r reveals triplet states; vibrational structure in the second triplet excited state.

Energy loss / eV	assignment	energy / meV (IR)
4.96	$1\nu_{6,7}(\delta_{C-H}$, A1)	132.16 / 123.36
5.09	$2\nu_{6,7}$	
5.22	$3\nu_{6,7}$	
5.34	$4\nu_{6,7}$	

Table C.1: Peak positions of the vibrational structure of the $^3A_1$ state.

$^1A_1$ ($a_2a_2^*$) that peaks at 7.80 eV according to previously reported UV spectra [120].

At residual energies as low as $E_r = 1$ eV (see figure C.2) the singlet transitions are suppressed and transitions from the singlet ground state to triplet states appear. The triplet transitions generally arise at lower energies than the corresponding singlet transitions. The two lowest states are ascribed to a $^3A_1$ state at 4.75 - 5.55 eV and a $^3B_2$ state at 3.4 - 4.65 eV and were reported previously [121]. The transition to the $^3A_1$ state exhibits clear vibrational structures [121], and are due to progression of the ν_6 or ν_7 vibrational mode (see tables C.1 - C.3). The presently observed peak positions are summarised in table C.1.

At 6 eV the $^1B_2$ state is still pronounced. Calculations using symmetry-adapter cluster configuration interaction (SAC-CI) predicted the 2^3A_1 state to be at 7.10 eV [122], which can be assigned to the structured peak at 6.3 - 6.9 eV. All other features cannot be assigned clearly.

Vibrational excitation By electron impact, basically all vibrational modes can be excited, but at small angles infrared allowed transitions are preferred. At incident electron energies that correspond to resonant negative ion states vibrations are more effectively excited via formation of a TNI and subsequent autodetachment. In this case excitation of higher vibrational levels is possible, i.e., overtones and combinational bands are observable. Resonant vibrational excitation of fu-

ran was measured by Motte-Tollet *et al.* [123], but only at energies around 6, 15 and 30 eV. A σ^* shape resonance was found at 6 eV by means of the excitation function of the C-H stretching mode. π^* shape resonances were observed in ETS measurements [124] at 1.73 eV (symmetry B1) and 3.15 eV (A2). A core excited resonance was found at 5.9 eV in DEA spectra [92, 91].

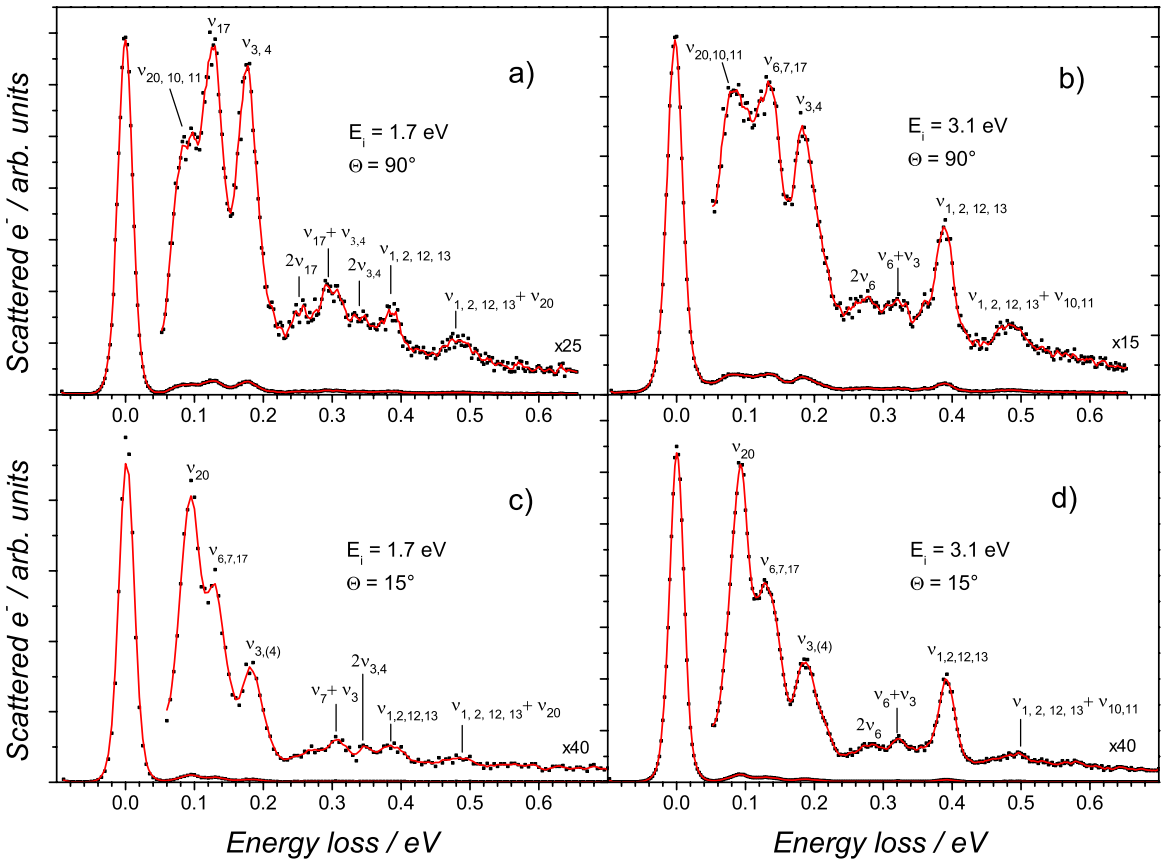

Figure C.3: Vibrational excitation of furan at $E_i = 1.7$ eV (a) and c)) and $E_i = 3.1$ eV (b) and d)).

In the present work resonant vibrational excitation is measured at incident energies of 1.7 and 3.1 eV, i.e., at the energies of the π^* shape resonances. The spectra are recorded in the electron energy loss mode, i.e., the incident energy E_i is fixed and the energy loss is recorded by varying the residual energy E_r. In figure C.3 the electron energy loss spectra are shown for the two incident energies (1.7 and

Energy loss / meV		vibration	energy / meV (IR)
$\theta = 90°$	$\theta = 15°$	(symmetry and mode)	
83 - 94 ± 2.5	96 ± 5	$\nu_{11}(\gamma_{ring}$, A2)	76.00
		$\nu_{10}(\gamma_{C-H}$, A2)	90.26
		$\nu_{20}(\gamma_{C-H}$, B2)	92.36 (VS)
126	130	$\nu_{7}(\delta_{C-H}$, A1)	123.36 (VS)
		$\nu_{17}(\delta_{ring}$, B1)	128.94 (shoulder)
		$\nu_{6}(\delta_{C-H}$, A1)	132.16 (S)
176	182	$\nu_{4}(\nu_{ring}$, A1)	171.59 (M)
		$\nu_{3}(\nu_{ring}$, A1)	184.86 (VS)
253		$2\nu_{7,17}$	
295	306	$\nu_{7,17}+ \nu_{4,3}$	
340	347	$2\nu_{4,3}$	
387	390	$\nu_{1,2}(\nu_{C-H}$, A1)	392.66 / 389.31
		$\nu_{12,13}(\nu_{C-H}$, B1)	391.91 / 387.95 (M)
481		$\nu_{1,2,12,13} + \nu_{10,11}$	

Table C.2: Assignment of vibrational excitations at $E_i = 1.7$ eV.

3.1 eV) and at scattering angles of 90° and 15°.

In tables C.2 and C.3 the assignment of vibrations is shown at the incident energies $E_i = 1.7$ eV and $E_i = 3.1$ eV, respectively. The observed bands are compared with vibrational modes obtained by IR spectroscopy [125].

Resonant vibrational excitation is more pronounced at large scattering angles. Below 200 meV bending modes are observed in all spectra. The assignment of the bands is not clear due to the energy resolution of 25 meV. At 1.7 eV two separated bands appear at 126 meV and 176 meV and a clear shoulder on the low energy side of the first band at 80 - 93 meV that are assigned to an in-plane bending ring mode (δ_{ring}), a ring stretching vibration (ν_{ring}) and out-of-plane bending C-

Energy loss / meV		vibration	energy / meV (IR)
$\theta = 90°$	$\theta = 15°$	(symmetry and mode)	
80 - 93 ± 2.5	93 ± 2.5	$\nu_{11}(\gamma_{ring}$, A2)	76.00
		$\nu_{10}(\gamma_{C-H}$, A2)	90.26
		$\nu_{20}(\gamma_{C-H}$, B2)	92.36 (VS)
123	129	$\nu_7(\delta_{C-H}$, A1)	123.36 (VS)
		$\nu_{17}(\delta_{ring}$, B1)	128.94 (shoulder)
135		$\nu_6(\delta_{C-H}$, A1)	132.16 (S)
181	188	$\nu_4(\nu_{ring}$, A1)	171.59 (M)
		$\nu_3(\nu_{ring}$, A1)	184.86 (VS)
273	281	$2\nu_6$	
319	320	$\nu_6 + \nu_3$	
387	391	$\nu_{1,2}(\nu_{C-H}$, A1)	392.66 / 389.31
		$\nu_{12,13}(\nu_{C-H}$, B1)	391.91 / 387.95 (M)
482	493	$\nu_{1,2,12,13} + \nu_{10,11}$	

Table C.3: Assignment of vibrational excitations at $E_i = 3.1$ eV.

H modes (γ_{C-H}). Between 200 meV and 350 meV overtones and combinational bands are observed. This is a clear evidence for a resonant vibrational excitation. At 387 meV the C-H stretching vibrations are excited.

In the spectrum at 3.1 eV the three low energy bands are clearly separated and slight differences in the energy positions are observed.

When a resonance state of the symmetry Γ is formed, vibrational modes belonging to the symmetry Γ or $\Gamma \times \Gamma$ are preferentially excited [126]. Hence it is expected that at 1.7 eV vibrations of the symmetry B1 and A1 are stronger excited, and at 3.1 eV the symmetries A1 and A2 are preferred. Furthermore ring modes should be preferred in contrast to C-H vibrations due to the charge distribution of the π^* orbitals [124].

In the case of furan excited at 1.7 eV the strong band at 126 meV is assigned to ν_{17} (δ_{ring}; 128 meV in IR) having symmetry B1 like its parent state. At 3.1 eV this band appears to be weaker and is slightly shifted to higher energies, and is hence attributed to ν_6 (δ_{C-H}; 132 meV in IR). The most striking difference is the strong excitation of the C-H stretching modes at 3.1 eV.

Going to smaller scattering angles the direct excitation becomes more important and dipole forbidden transitions are less likely. In figure C.3 c) and d) the vibrational excitation spectra are displayed at a scattering angle $\theta = 15°$. Both spectra are very similar confirming that the resonance mechanism becomes less dominant. Nevertheless the ν_{C-H} vibrations are still very strong at 3.1 eV.